1-^{11}C-Acetate Versus ^{18}F-FDG PET in Detection of Meningioma and Monitoring the Effect of γ-Knife Radiosurgery

Ren-Shyan Liu[1–3], Chen-Pei Chang[2], Wen-You Guo[4], David H.C. Pan[5], Donald Ming-Tak Ho[6], Chi-Wei Chang[1], Bang-Hung Yang[1,3], Liang-Chi Wu[1,2], and Shin-Hwa Yeh[1,2]

[1]Department of Nuclear Medicine, National PET/Cyclotron Center, Taipei Veterans General Hospital, Taipei, Taiwan; [2]Molecular and Genetic Imaging Core, National Yang-Ming University Medical School, Taipei, Taiwan; [3]Department of Biomedical Imaging and Radiological Sciences, National Yang-Ming University, Taipei, Taiwan; [4]Department of Radiology, Taipei Veterans General Hospital, Taipei, Taiwan; [5]Department of Neurosurgery, Institute of Neurology, Taipei Veterans General Hospital, Taipei, Taiwan; and [6]Department of Pathology, Taipei Veterans General Hospital, Taipei, Taiwan

This study aimed to define the potential of 1-^{11}C-acetate PET, compared with ^{18}F-FDG, in detecting meningiomas and monitoring the effect of γ-knife radiosurgery. **Methods:** Twenty-two patients with the neuroradiologic diagnosis of meningioma were examined by 1-^{11}C-acetate and ^{18}F-FDG PET on the same day. There were 12 cases of histopathologically proven meningioma (8 grade I, 2 grade II, and 2 grade III), 1 of tuberculous granuloma, and 1 of degenerative tissue. 1-^{11}C-acetate PET scans of fasting patients were obtained 10 min after intravenous administration of 740 MBq of 1-^{11}C-acetate. ^{18}F-FDG PET was performed at 2 h after 1-^{11}C-acetate scanning. The PET images were evaluated by a qualitative method and semiquantitative analysis using standardized uptake value and tumor-to-cortex ratio. **Results:** The ^{18}F-FDG PET study revealed a hypometabolic focus in 17 meningiomas (8 grade I, 1 grade II, and 8 unknown grade) and hypermetabolism in 1 grade II and 2 grade III meningiomas. High uptake of 1-^{11}C-acetate was observed in all 20 meningiomas, in contrast to the low uptake in surrounding normal brain tissue, allowing a clearer demarcation of the tumor boundary than that provided by ^{18}F-FDG. Dissociation of regional accumulation of 1-^{11}C-acetate and ^{18}F-FDG within the tumor was also noted on the coregistered images. The standardized uptake value for 1-^{11}C-acetate was not different from that for ^{18}F-FDG (mean ± SD, 3.16 ± 1.75 vs. 3.22 ± 1.50, P = 0.601), but the tumor-to-cortex ratio for 1-^{11}C-acetate was higher than that for ^{18}F-FDG (3.46 ± 1.38 vs. 0.93 ± 1.08, $P < 0.005$). ^{18}F-FDG was able to differentiate grade I from grade II–III meningiomas, whereas 1-^{11}C-acetate was unable to do so. Tuberculous granuloma had a high 1-^{11}C-acetate and ^{18}F-FDG uptake similar to that of grade II/III meningioma. Five patients received 1-^{11}C-acetate and ^{18}F-FDG PET before and after γ-knife surgery. 1-^{11}C-acetate performed better than did ^{18}F-FDG in monitoring the response of tumor metabolism to radiosurgery. **Conclusion:** 1-^{11}C-acetate was found to be useful for detecting meningiomas and evaluating the extent of meningiomas and potentially useful for monitoring tumor response to radiosurgery. However, 1-^{11}C-acetate was not useful for evaluating the tumor grade. ^{18}F-FDG was found to be less useful than 1-^{11}C-acetate for evaluating the extent of meningiomas and the response to radiosurgical treatment but may be useful for differentiating benign from malignant meningiomas. ^{18}F-FDG and 1-^{11}C-acetate are complementary for assessing diverse cell metabolism of meningioma.

Key Words: 1-^{11}C-acetate; ^{18}F-FDG; meningioma; positron emission tomography; radiosurgery

J Nucl Med 2010; 51:883–891
DOI: 10.2967/jnumed.109.070565

Meningioma is a common, usually benign, solitary tumor of the meninges, constituting about 15% of all primary brain tumors (*1*). Histopathologically, meningiomas are divided into 3 malignancy grades: benign, atypical, and anaplastic meningiomas (*2*). Surgery is the primary treatment of meningioma; however, meningioma is not always curable. The atypical and anaplastic forms are associated with a high risk of recurrence (*2*). The rate of recurrence depends on the completeness of removal, the site of the tumor, and its biologic aggressiveness (*3*). Postoperative radiotherapy for preventing the recurrence of benign meningiomas after partial resection and radiosurgery for small meningiomas has been accepted by neurosurgeons (*4,5*). Radiosurgery may stop the growth of meningioma and sometimes even lead to a decrease in the size of the tumor (*5*). Control of tumor growth in most cases means unchanged tumor volume rather than decrease in volume (*5*); therefore, it is difficult to assess the effect of treatment by measuring the change of the tumor size by CT or MRI.

^{18}F-FDG has been proven useful for the detection of brain tumors, histologic grading of the tumor, and differentiation of recurrent high-grade tumors from radiation- or chemotherapy-induced necrosis (*6,7*). The application of

Received Sep. 9, 2009; revision accepted Feb. 16, 2010.
For correspondence or reprints contact: Ren-Shyan Liu, Department of Nuclear Medicine, National Yang-Ming University and Taipei Veterans General Hospital, 201, Sec. 2, Shih-Pai Rd., Taipei, Taiwan 112.
E-mail: rsliu@vghtpe.gov.tw

^{18}F-FDG is based on an increased glycolysis and deficient respiratory rate in neoplastic cells (*8,9*). Meningiomas have been found to have high ^{18}F-FDG accumulation, equivalent to that of the cortical gray matter or low glucose metabolism (*10,11*). Glucose consumption of meningioma assessed by ^{18}F-FDG PET has been proposed as an index of tumor aggressivity and probability of recurrence (*11*). Atypical meningioma had the highest glucose use rate, followed by papillary meningioma and angioblastic meningioma (*11*). Significantly, elevated ^{18}F-FDG uptake in grades II and III, compared with grade I, meningiomas has also been reported (*12*). Recurrent meningiomas had higher glucose use rates demonstrated by ^{18}F-FDG PET than primary tumors (*11*). Although ^{18}F-FDG PET was thought to be useful for detecting the meningiomas and evaluating the degree of malignancy, contradictory results have also been reported. Cremerius et al. found that for most primary or recurrent meningiomas, especially grade I tumors, ^{18}F-FDG is not an ideal tracer to delineate the tumor (*12,13*). Within the brain, demarcation of meningiomas and related edema may be difficult because of lower glucose consumption than in normal brain (*11*).

Radiolabeled amino acid is an alternative to ^{18}F-FDG for the localization of meningiomas. Meningiomas have a relatively high uptake ratio of ^{11}C-L-methionine, and thus the tumors could be well delineated from normal brain tissue (*14*). ^{11}C-tyrosine is another valid amino acid for use in diagnosis of brain tumors. Several studies have demonstrated the benefit of *O*-(2-^{18}F-fluoroethyl)-L-tyrosine PET in the diagnosis of gliomas and delineation of tumor borders when a combination of MRI and *O*-(2-^{18}F-fluoroethyl)-L-tyrosine PET was used (*15*). However, there were controversial reports on the uptake of ^{11}C-tyrosine by meningiomas (*16*). ^{11}C-choline has also been proven useful for the detection of malignant and benign brain tumors (*17*). The accumulation of ^{11}C-choline was high in benign tumors (i.e., meningiomas, neurinomas, and hemangioblastomas), whereas the uptake of ^{18}F-FDG by these tumors was low (*17*).

1-^{11}C-acetate has been used for the detection of renal carcinoma (*18*), nasopharyngeal carcinoma (*19*), prostate cancer (*20*), hepatoma (*21*), and astrocytoma (*22*). The possible mechanisms of tumor uptake of 1-^{11}C-acetate include impaired tricarboxylic acid cycle activity or the distribution of tracer among the various intermediate metabolites (*19*) or incorporation of tracer in the tumor through the anabolic pathways in fatty acid and sterol synthesis (*20*). Dienel et al. reported that 2-^{14}C-acetate preferentially labeled glial tumors grown in rat brain and human glioma and meningioma explants (*23*). Our previous study showed that 1-^{11}C-acetate detected astrocytomas better than did ^{18}F-FDG (*22*). No clinical studies have so far compared 1-^{11}C-acetate and ^{18}F-FDG PET in the diagnosis of meningioma. This study aimed to assess the usefulness of 1-^{11}C-acetate, compared with ^{18}F-FDG, for the evaluation of the extent and the histologic grade of meningioma and to evaluate the usefulness of these tracers for monitoring tumor response to radiosurgery.

MATERIALS AND METHODS

Patients

We evaluated 22 patients (10 men, 12 women; mean age, 56.7 y; age range, 35–81 y) with meningiomas or suspected meningiomas. All patients were examined by 1-^{11}C-acetate and ^{18}F-FDG PET on the same day. The patient characteristics are summarized in Table 1. In 14 patients, pathologic diagnosis was obtained by tumor resection or biopsy after PET examination. Among them, there were 12 meningiomas, 1 tuberculous granuloma, and 1 degeneration with necrotic and fibrotic tissues. In 8 patients for whom no results of pathologic examinations could be obtained, the diagnosis of meningioma was based on radiologic and clinical investigation. According to the World Health Organization classification of brain tumors (*24*) and the histopathologic criteria for diagnosis of malignant meningioma (*25*), 8 meningiomas were classified grade I (benign), 2 grade II (atypical), and 2 grade III (malignant). Five patients received both 1-^{11}C-acetate and ^{18}F-FDG PET scans before and 6–35 mo after γ-knife radiosurgery (Elekta Instrument), with the target dose ranging from 28 to 40 Gy. This study was approved by the institutional ethics committee, and informed consent was obtained from all patients.

Radiopharmaceutical Preparation

The 1-^{11}C-acetate was synthesized by carbonation of Grignard reagent. ^{11}C-carbon dioxide was reacted with 0.15 M methylmagnesium bromide and hydrolyzed with 0.4 M hydrochloric acid to convert to 1-^{11}C-acetate acid (*26*). All reaction steps were performed by a robotic system (Scanditronix Anatech RBIII) controlled by a computer. The radiochemical purity was greater than 99%. ^{18}F-FDG was synthesized following the method described in the literature (*27*).

PET Procedures

PET images were acquired with a PC-4096 PET (Scanditronix AB) or an ECAT HR+ PET scanner (Siemens-CTI). The primary imaging parameters of the PC-4096 PET scanner were in-plane and axial resolution of 5.6 mm in full width at half maximum and 15 contiguous slices separated by 6.5 mm. The ECAT HR+ scanner allowed simultaneous acquisition of 63 contiguous cross-sectional slices with 2.4-mm slice thickness. Axial and in-plane resolution of the ECAT HR+ scanner was 2.4 mm in full width at half maximum. Transmission scanning was performed with a ^{68}Ga pin source to correct for photon attenuation. PET scans were obtained from patients who had fasted. The patient's head was positioned and fixed with the detector parallel to the orbitomeatal line. 1-^{11}C-acetate (740 MBq [20 mCi]) was injected intravenously, and a 20-min emission scan was obtained at 10 min after injection (*22*). ^{18}F-FDG was performed at 2 h after completion of the 1-^{11}C-acetate scan. At 45 min after intravenous injection of 370 MBq (10 mCi) of ^{18}F-FDG, a 20-min emission scan was obtained. Tomographic images obtained from the PC-4096 PET scanner were reconstructed with a 128 × 128 matrix by filtered backprojection using a Hanning filter (cutoff frequency, 0.5 Nyquist; order, 8). Images obtained from the ECAT HR+ scanner were reconstructed with a 128 × 128 matrix by the ordered-subset expectation maximization (iterations, 2; subset, 8).

TABLE 1. Clinical Data, Pathology, and PET Results

Patient no.	Age (y)	Sex	Primary or recurrent	Location of tumor	Method of diagnosis	Histology subtype/associated grade	SUV_{ACE}	$SUV_{^{18}F\text{-}FDG}$	T/C_{ACE}	$T/C_{^{18}F\text{-}FDG}$
1	77	M	Primary	L lateral ventricle	Rad/clin	N/A	2.89	4.00	2.60	0.59
2	37	F	Primary	L CPA	Rad/clin	N/A	4.20	3.59	4.13	0.53
3	59	F	Primary	R parasellar	Rad/clin	N/A	4.10	2.03	4.31	0.41
4	58	M	Primary	R CPA	Rad/clin	N/A	1.87	3.11	2.35	0.64
5	56	M	Primary	R parietal, L parietal	Surgery	Meningothelial/I	3.06	3.44	3.82	0.67
6	55	F	Primary	L sphenoid ridge	Surgery	Transitional/I	3.86	2.54	4.47	0.72
7	46	F	Primary	L CPA	Surgery	Transitional/I	1.74	1.15	2.26	0.27
8	51	F	Primary	R CPA	Surgery	Atypical/II	2.67	2.39	4.38	0.69
9	35	M	Primary	Clivus	Surgery	Transitional/I	5.80	1.54	5.50	0.70
10	43	F	Primary	L CPA	Surgery	Meningothelial/I	2.16	2.30	2.90	0.56
11	58	F	Primary	L CPA	Surgery	Transitional/I	2.74	3.28	2.45	0.47
12	53	F	Primary	R parietal	Surgery	Transitional/I	1.46	3.18	1.91	0.88
13	55	M	Primary	L frontal, parietal	Surgery	Malignant melanoma/III	4.35	6.08	5.57	1.59
14	79	M	Recurrent	R parietal	Surgery	Atypical/II	1.20	4.38	3.41	1.80
15	47	F	Recurrent	L parietal	Surgery	Transitional/I	1.17	1.38	1.23	0.67
16	63	M	Recurrent	L skull base	Surgery	Anaplastic/III	4.57	6.47	4.84	5.23
17	66	F	Recurrent	R petroclival	Rad/clin	N/A	4.15	5.32	3.25	0.69
18	81	M	Recurrent	R lateral ventricle	Rad/clin	N/A	0.88	3.81	1.99	0.47
19	41	F	Recurrent	L trigone	Rad/clin	N/A	2.34	1.43	1.89	0.38
20	72	M	Recurrent	L petroclival	Rad/clin	N/A	7.94	3.07	5.86	0.70
21	54	F		R sphenoid ridge	Surgery	Degeneration, necrosis, and fibrosis	1.31	2.44	1.30	0.42
22	62	M		Parietal (falx)	Biopsy	Tuberculous granuloma	3.11	7.63	2.41	1.52

SUV_{ACE} = SUV of 1-^{11}C-acetate; $SUV_{^{18}F\text{-}FDG}$ = SUV of ^{18}F-FDG; T/C_{ACE} = T/C of 1-^{11}C-acetate; $T/C_{^{18}F\text{-}FDG}$ = T/C of ^{18}F-FDG; Rad/clin = radiologic/clinical diagnosis; N/A = not available; CPA = cerebelopontine angle.

Image and Data Analysis

The 1-^{11}C-acetate and ^{18}F-FDG uptake of the tumors was evaluated by both qualitative and semiquantitative methods. For qualitative analysis, the degree of tracer uptake by the tumor was evaluated visually by comparing with tracer uptake by the cerebral cortex contralateral to the tumor without any morphologic abnormalities on MRI (*28*). Tracer uptake by the tumor clearly lower than that of the contralateral cortex was interpreted as hypometabolic, whereas tumor tracer uptake equal to or clearly higher than that of the contralateral cortex was interpreted as hypermetabolic. For semiquantitative analysis, regions of interest (ROIs) were selected manually with the reference of PET and MR images. The ROIs of the tumors were squares measuring from 12 × 12 mm to 20 × 20 mm that included the highest activity area and did not cover the entire tumor. A same ROI was then placed on the contralateral corresponding region. In cases without significant tracer uptake by the tumors, the ROIs were defined using the MR image as a reference. The mean pixel values in the ROIs were used for the quantitative analysis. The tracer uptake was measured using standardized uptake value (SUV) as SUV = radioactivity in ROI (Bq/mL) per injected dose (Bq) per body weight (g). Tumor-to-cortex (T/C) uptake ratio was determined as the ratio of SUV of the tumor to the contralateral corresponding region of cerebral cortex (*29*).

Statistical Analysis

The differences in SUVs between 1-^{11}C-acetate and ^{18}F-FDG and in T/C ratios between 1-^{11}C-acetate and ^{18}F-FDG were analyzed by Wilcoxon signed rank test. The differences in the SUVs of 1-^{11}C-acetate and ^{18}F-FDG and in the T/C ratios of 1-^{11}C-acetate and ^{18}F-FDG between grade I and grades II–III meningiomas and between primary and recurrent meningiomas were analyzed by Mann–Whitney rank sum test. Correlation of SUVs of 1-^{11}C-acetate and ^{18}F-FDG and of T/C ratios of 1-^{11}C-acetate and ^{18}F-FDG was tested by simple regression analysis. The significance of the linear regression was tested by ANOVA. A P value of less than 0.05 was considered to represent a significant difference between the values tested. The statistical analysis was performed using SPSS software (version 17.0; SPSS Inc.).

RESULTS

All 20 meningiomas had enhanced 1-^{11}C-acetate uptake, allowing a good contrast to the surrounding normal brain tissues with low 1-^{11}C-acetate uptake (Fig. 1). In the ^{18}F-FDG PET study, only 3 high-grade meningiomas (grades II–III) were hypermetabolic, with ^{18}F-FDG uptake higher than or equal to the contralateral normal cortex (Fig. 2). The remaining 17 meningiomas (8 grade I, 1 grade II, and 8 unknown grade) were hypometabolic. The results of the PET studies are shown in Table 1. The SUV of 1-^{11}C-acetate was not different from that of ^{18}F-FDG (mean ± SD, 3.16 ± 1.75 vs. 3.22 ± 1.50, P = 0.601), but the T/C ratio of 1-^{11}C-acetate was higher than that of ^{18}F-FDG

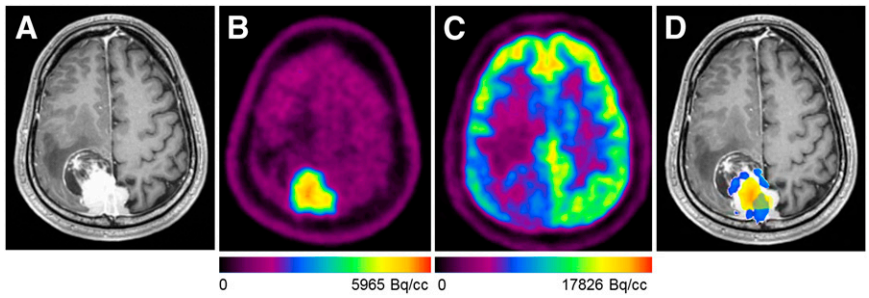

FIGURE 1. Patient 4, meningothelial meningioma (grade I). (A) MR image (T1-weighted image after gadolinium injection) showing necrotic lesion with heterogeneous contrast enhancement in right parietal region. (B and C) PET images showing high uptake of 1-^{11}C-acetate (SUV, 3.06; T/C ratio, 3.82) (B) but low uptake of ^{18}F-FDG (SUV, 3.44; T/C ratio, 0.67) (C) in tumor. (D) When PET images obtained with the 2 tracers were coregistered, foci of ^{18}F-FDG uptake (blue) corresponded to regions of low 1-^{11}C-acetate uptake (yellow). Nearly no overlay of blue color foci on hot spot of 1-^{11}C-acetate (red) is seen.

(3.46 ± 1.38 vs. 0.93 ± 1.08, $P < 0.005$). The meningiomas were better delineated by 1-^{11}C-acetate than by ^{18}F-FDG because of low acetate uptake in the normal cortex. The correlation of the SUVs of 1-^{11}C-acetate and ^{18}F-FDG and the correlation of the T/C ratios of 1-^{11}C-acetate and ^{18}F-FDG were poor ($r^2 = 0.031$, $P = 0.430$, and $r^2 = 0.104$, $P = 0.144$, respectively) (Fig. 3). SUV and T/C of 1-^{11}C-acetate uptake were not useful for differentiating low-grade (I) from high-grade (II–III) meningiomas ($P = 0.683$ and $P = 0.109$, respectively), whereas the T/C ratio of ^{18}F-FDG uptake was better than that of 1-^{11}C-acetate for differentiating grade I from grades II–III meningiomas ($P = 0.026$) (Table 2; Fig. 4A). SUVs of ^{18}F-FDG uptake in grade I meningiomas were also lower than those of grades II–III tumors ($P = 0.048$). There was no significant difference in the T/C ratios of 1-^{11}C-acetate and ^{18}F-FDG ($P = 0.536$ and $P = 0.473$, respectively) or in the SUVs of 1-^{11}C-acetate and ^{18}F-FDG ($P = 0.643$ and $P = 0.438$, respectively) between primary and recurrent meningiomas (Table 3; Fig. 4B).

Coregistration of PET images of the 2 tracers and the MR image with differential color-coding of corresponding ^{18}F-FDG (blue) and 1-^{11}C-acetate images (yellow and red) revealed the spatial dissociation of ^{18}F-FDG and 1-^{11}C-acetate accumulation in meningiomas (Figs. 1D and 2D). The foci of highest ^{18}F-FDG uptake (blue) corresponded to the regions of low 1-^{11}C-acetate (yellow) within the tumor. Nearly no overlay of foci with enhanced ^{18}F-FDG uptake (blue) on the zones of highest 1-^{11}C-acetate uptake (red) was observed.

A case of suspected recurrent meningioma (patient 21) and a case of suggestive falx meningioma (patient 22) were finally proven to be degenerative tissue with necrosis and fibrosis without evidence of tumor recurrence and a chronic granulation inflammation, compatible with meningeal tuberculous granuloma, respectively. The T/C ratio of 1-^{11}C-acetate of the degenerative lesion (1.81) was within the range of that of grade I meningioma (1.64–4.5, mean ± SD), and the T/C ratio of ^{18}F-FDG (0.92) was slightly higher than the upper limit of the range of that of the low-grade meningiomas (0.44–0.80, mean ± SD). The T/C ratio of 1-^{11}C-acetate uptake of the meningeal tuberculosis was 4.02, which is in the range of grades II–III meningiomas (3.65–5.45), and the T/C ratio of ^{18}F-FDG uptake (3.86) was also in the range of grades II–III meningiomas (0.34–4.32) (Fig. 5).

Five patients underwent MRI and 1-^{11}C-acetate and ^{18}F-FDG PET examinations before and after γ-knife surgery (Fig. 6). Compared with the baseline data before radiosurgery, the percentage changes of tumor volume and the T/C ratios of 1-^{11}C-acetate and ^{18}F-FDG uptake for each follow-up examination were calculated. Follow-up examinations of 4 patients (patients 2–5) within 1 y after radiosurgery revealed reduced tumor volume in patient 2, no change of volume in patients 3 and 5, and increased volume in patient 4. The T/C ratio of 1-^{11}C-acetate was reduced and

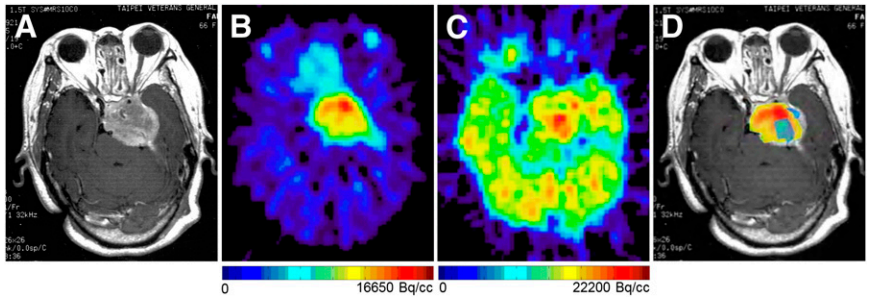

FIGURE 2. Patient 16, anaplastic meningioma (grade III). (A) Contrast-enhanced MR image showing necrotic lesion in middle fossa of left skull base. (B and C) PET images show increased uptake of both 1-^{11}C-acetate (SUV, 4.57; T/C ratio, 4.84) (B) and ^{18}F-FDG (SUV, 6.47; T/C ratio, 5.23) (C) in tumor. (D) Coregistered PET image obtained with the 2 tracers showed that highest foci of ^{18}F-FDG uptake (blue) corresponded to regions of low 1-^{11}C-acetate uptake (yellow). No obvious overlay of blue color foci on hot spot of 1-^{11}C-acetate (red) is seen.

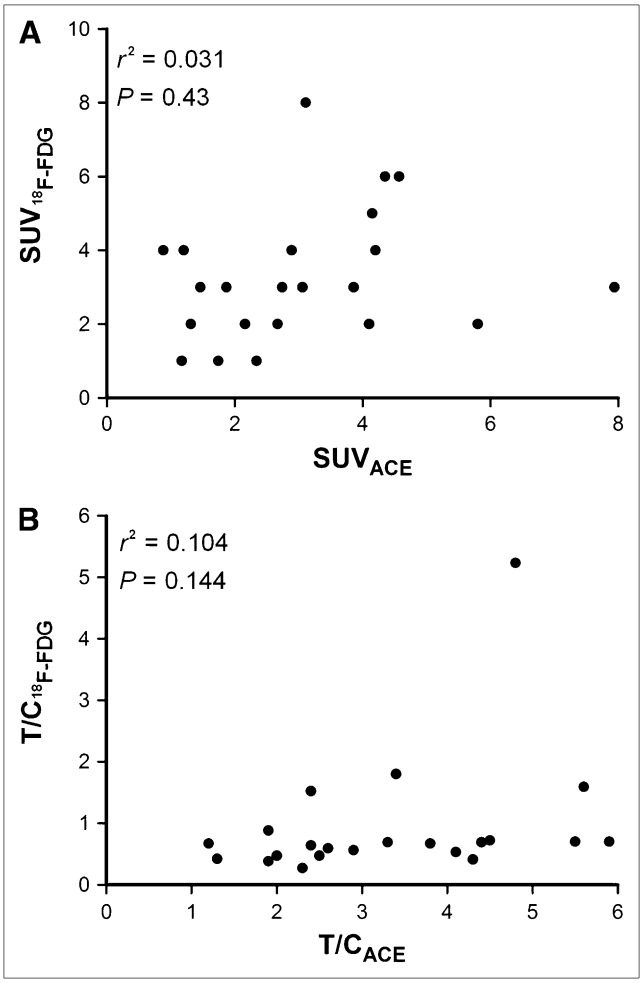

FIGURE 3. Regression analysis of SUVs of 1-^{11}C-acetate (SUV_{ACE}) vs. 18F-FDG ($SUV_{^{18}F\text{-}FDG}$) (A) and T/C ratios of 1-^{11}C-acetate uptake (T/C_{ACE}) vs. ^{18}F-FDG uptake ($T/C_{^{18}F\text{-}FDG}$) (B). Correlations were poor.

the T/C ratio of ^{18}F-FDG was increased in all 4 patients. Patients 1–3 were followed by PET studies longer than 1 y. Tumor volume and T/C ratios of 1-^{11}C-acetate and ^{18}F-FDG, compared with the preradiosurgery baseline data, were reduced. Patient 2 showed reduced tumor volume and 1-^{11}C-acetate uptake but increased ^{18}F-FDG uptake at 6 and 12 mo after radiosurgery. At the 35th month, the ^{18}F-FDG uptake decreased and the tumor volume and 1-^{11}C-acetate uptake further decreased. Patient 3 showed no change of tumor volume, increased ^{18}F-FDG uptake, and decreased 1-^{11}C-acetate uptake at 8 mo after radiosurgery; decreased tumor volume, ^{18}F-FDG uptake, and further decreased 1-^{11}C-acetate uptake were observed at 14 mo (Fig. 7). In patient 4, only 1-^{11}C-acetate PET showed a response to radiosurgery at 6 mo. Reduction of tumor volume was noted 12 mo later. Increased ^{18}F-FDG uptake in the early follow-up PET may be caused by postradiation inflammation or adverse radiation effect. The 1-^{11}C-acetate PET scan better demonstrated reduction of tumor metabolism after radiosurgery than did the ^{18}F-FDG PET scan, and the change of the T/C ratio of 1-^{11}C-acetate was better than that of ^{18}F-FDG and tumor volume for reflecting the therapeutic response, especially in the early follow-up at 6 mo after radiosurgery.

DISCUSSION

Our results showed that all meningiomas were hypometabolic for ^{18}F-FDG except an anaplastic meningioma, an atypical meningioma, and a primary meningeal malignant melanoma, which were hypermetabolic. All meningiomas had high uptake of 1-^{11}C-acetate in contrast to low uptake in normal brain tissue, allowing a good delineation of the tumors. SUVs and T/C ratios of ^{18}F-FDG in grades II–III meningiomas were higher than those in grade I tumors, but SUVs and T/C ratios of 1-^{11}C-acetate were not. ^{18}F-FDG better differentiated grade I from grades II–III meningiomas than did 1-^{11}C-acetate. The 1-^{11}C-acetate and ^{18}F-FDG uptake of recurrent meningiomas was not significantly different from that of the primary tumor, although the mean SUV and T/C of ^{18}F-FDG of recurrent meningiomas looked higher than that of primary tumor.

In the brain, acetate is preferentially metabolized by astrocytes, and labeled acetate has been used to assess glial metabolism and glial–neuronal interactions (*23*). Metabolic data derived from a small set of tumors revealed that glioblastoma and meningioma clearly can convert ^{14}C-acetate into acidic and amino acid metabolites, presumably through the oxidative pathway of the tricarboxylic acid cycle (*23*). The rate of metabolism of acetate in the normal rat brain is lower and more homogeneous than the local rates of glucose use (*23,30*) and slightly increases during

TABLE 2. Comparison of 1-^{11}C-Acetate and ^{18}F-FDG Uptake Between Low-Grade (I) and High-Grade (II–III) Meningiomas

Grade	SUV_{ACE}	$SUV_{^{18}F\text{-}FDG}$	T/C_{ACE}	$T/C_{^{18}F\text{-}FDG}$
I (n = 8)	2.75 ± 1.52*	2.35 ± 0.91	3.07 ± 1.43	0.62 ± 0.18
II/III (n = 4)	3.20 ± 1.58	4.83 ± 1.86	4.55 ± 0.90	2.33 ± 1.99
P	0.683	0.048	0.109	0.026

*Data are mean ± SD.
SUV_{ACE} = SUV of 1-^{11}C-acetate; $SUV_{^{18}F\text{-}FDG}$ = SUV of ^{18}F-FDG; T/C_{ACE} = T/C of 1-^{11}C-acetate; $T/C_{^{18}F\text{-}FDG}$ = T/C of ^{18}F-FDG.

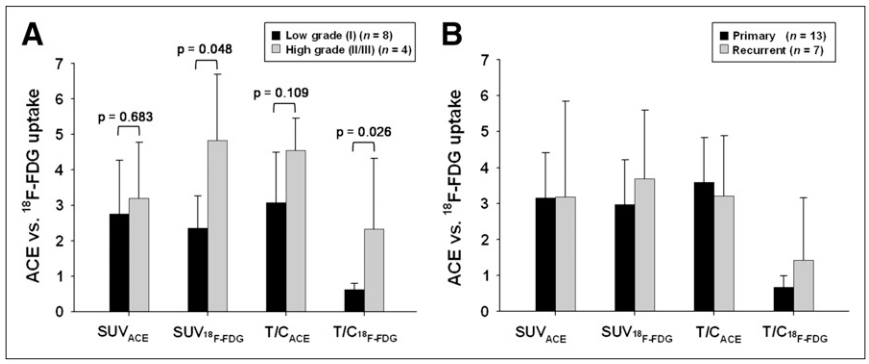

FIGURE 4. Statistical significance of 1-^{11}C-acetate and ^{18}F-FDG uptake between low-grade (I) and high-grade (II–III) meningiomas (A) and between primary and recurrent meningiomas (B). Data represent mean ± SD. ACE = 1-^{11}C-acetate.

physiologic stimulation (*31,32*). This advantage of radiolabeled acetate provides a stable low background and higher T/C ratio to delineate the meningioma.

In the study by Dienel et al., 2-^{14}C-acetate was used instead of 1-^{14}C-acetate so that less ^{14}C would be lost through decarboxylation reactions (*23*). Because of the loss of contrast between normal and abnormal tissue due to efflux or spreading of labeled metabolites, the experimental period in the study by Dienel et al. was only 5 min to minimize product loss and spreading (*23*). In the brain tissue of a cat, 1-^{14}C-acetate quickly incorporated into glutamate and glutamine (*33*). ^{14}C incorporated into these amino acids, and total radioactivity in the brain rose for at least 15 min and then fell by 30 min. With increasing time, progressively higher amounts of ^{14}C-acetate would be incorporated into protein and lipid (*33*). We have studied previously the use of 1-^{11}C-acetate PET for the detection of astrocytoma (*22*). The results showed all 41 astrocytomas (8 low grade and 33 high grade) had enhanced uptake of 1-^{11}C-acetate, with high contrast to normal brain tissue, whereas ^{18}F-FDG PET detected hypermetabolic lesions in 47% of anaplastic astrocytomas, in 88% of glioblastomas, and in none of the low-grade astrocytomas (*22*). Our current study also showed a high contrast of uptake of 1-^{11}C-acetate between meningioma and normal brain tissue. 1-^{11}C-acetate PET images were obtained from 10 to 30 min after administration of the radiotracer. The contrast between normal brain tissue and meningioma obtained by our method was high enough to delineate the tumor. Obviously, loss of ^{11}C through decarboxylation reactions did not defer the detection of meningioma by PET. Although carbons in position 2 of acetyl-CoA are more likely directed toward gluconeogenesis and incorporation into glutamine (*34*), glutamine isotopic enrichment is slightly but not significantly higher when 1-^{13}C-acetate is infused, versus 2-^{13}C-acetate (*35*). These findings may support the adequacy of the use of 1-^{11}C-acetate as a PET agent for detecting meningiomas.

^{18}F-FDG and 1-^{11}C-acetate uptakes in meningioma are heterogeneous. Interestingly, most of the regions in the meningiomas with low ^{18}F-FDG uptake had enhanced uptake of 1-^{11}C-acetate (Figs. 1 and 2). This dissociation of ^{18}F-FDG and 1-^{11}C-acetate uptake in the tumors was well demonstrated in the coregistered PET images of the 2 tracers and MR image (Figs. 1D and 2D). Although tumor glycolysis and lactate efflux might stimulate acetate uptake into astrocytes (*36*), Dienel et al. disclosed that spreading depression caused heterogeneous increases in labeling of the cerebral cortex with acetate, butyrate, and deoxyglucose, and the monocarboxylic acid uptake was highest in the structures in which apparent loss of labeled metabolites of 6-^{14}C-glucose was greatest (*37*). A previous study on the cell lines of colon adenocarcinoma, ovary carcinoma, and malignant melanoma revealed higher tumor-to-normal ratios of 1-^{14}C-acetate than of 2,6-3H-2-deoxy-glucose, mainly because of the enhanced lipid synthesis of cell membrane, which reflects the high growth activity of neoplasms (*38*). Clinical studies of prostate cancer (*39*) were concordant with these findings. The preferential metabolism of acetate to the membrane lipids in tumor cells for the constitution of membrane for cell growth and proliferation may also partly explain the discrepantly high acetate uptake in meningioma (*38*). Cytosolic acetyl-CoA synthetase plays an important role in the tumor uptake of

TABLE 3. Comparison of 1-^{11}C-Acetate and ^{18}F-FDG Uptake Between Primary and Recurrent Meningiomas

Meningiomas	SUV_{ACE}	$SUV_{^{18}F\text{-}FDG}$	T/C_{ACE}	$T/C_{^{18}F\text{-}FDG}$
Primary (n = 13)	3.15 ± 1.26*	2.97 ± 1.25	3.59 ± 1.25	0.67 ± 0.32
Recurrent (n = 7)	3.18 ± 2.67	3.69 ± 1.90	3.21 ± 1.68	1.42 ± 1.74
P	0.643	0.438	0.536	0.473

*Data are mean ± SD.
SUV_{ACE} = SUV of 1-^{11}C-acetate; $SUV_{^{18}F\text{-}FDG}$ = SUV of ^{18}F-FDG; T/C_{ACE} = T/C of 1-^{11}C-acetate; $T/C_{^{18}F\text{-}FDG}$ = T/C of ^{18}F-FDG.

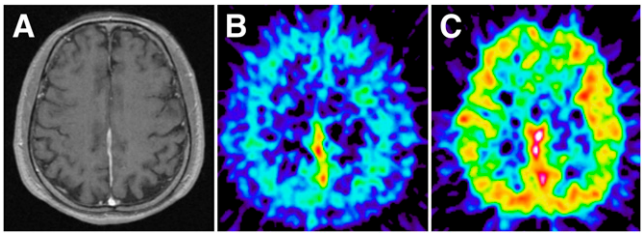

FIGURE 5. Patient 22, meningeal tuberculosis. (A) MR image showing contrast enhancement along falx in parietal region. (B and C) PET images showing enhanced uptake of both 1-^{11}C-acetate (SUV, 3.11; T/C ratio, 2.41) (B) and ^{18}F-FDG (SUV, 7.63; T/C ratio, 1.52) (C) in lesion.

radiolabeled acetate (*40*); it is a bidirectional enzyme that controls acetyl-CoA–acetate metabolism in tumor cells (*40*). The uptake of radiolabeled acetate in tumors along with upregulation of cytosolic acetyl-CoA synthetase expression increased under hypoxia (*40*). The heterogeneity and dissociation of regional distribution of ^{18}F-FDG and 1-^{11}C-acetate in meningioma suggest the diverse metabolic behavior within the meningioma. There are zones of cells with abundant cytosol acetyl-CoA synthetase and dominant use of acetate for the synthesis of glutamine and lipid and energy metabolism, and there are zones of cells with dominant glycolysis as part of energy metabolism. The results of the current study indicate the potential role of 1-^{11}C-acetate to evaluate the cell growth of meningioma and, in combination with ^{18}F-FDG, to characterize the cellular properties of the tumor.

Our current study also revealed that 1-^{11}C-acetate was unable to differentiate grade I from grades II–III meningiomas. Unlike 1-^{11}C-acetate, ^{18}F-FDG accumulated more in the grades II–III meningiomas than in the grade I tumors, which is compatible with the results reported by Cremerius et al. (*13*). ^{18}F-FDG uptake is a more accurate reflection of tumor grade than is 1-^{11}C-acetate uptake.

Experiences with ^{18}F-FDG PET–guided biopsy have shown that targeting may be difficult when there is low ^{18}F-FDG uptake in low-grade tumors and when a hypermetabolic tumor is near the cortical or subcortical gray matter (*41*). ^{11}C-methionine has been considered more suitable than ^{18}F-FDG for delineating the boundary of brain tumor (*29,41*) because its uptake is increased in low-grade gliomas but is low in gray matter, providing a more sensitive signal than ^{18}F-FDG for PET-guided neurosurgical procedures in gliomas (*42*). 1-^{11}C-acetate has the same merit as ^{11}C-methionine, for example, high uptake in low-grade gliomas (*22*) and meningiomas and low uptake in gray matter, resulting a good contrast in delineating tumor extent. 1-^{11}C-acetate might be an alternative to ^{18}F-FDG and ^{11}C-methionine in delineating the entire volume of meningioma for stereotactic biopsy.

The increased application of radiosurgery in the treatment of meningiomas has created a demand for higher precision in diagnostic imaging in pretreatment planning for postoperative tumor remnants or recurrences (*14,43,44*). The traditional criteria for the assessment of surgical results—eradication of the tumor—cannot be applied in radiosurgery, and arrest of tumor growth is considered a success (*43*). A short period of postradiosurgical observation may erroneously assess an unchanged size of the tumor as a result of the treatment, because no change in the tumor size occurred in most of the cases (*43*). PET may provide an ideal tool to explore the biologic changes of the tumor after radiosurgery. The high contrast against the surrounding tissue in all meningiomas in our series is promising that 1-^{11}C-acetate PET may facilitate more proper tumor identification and delineation and thereby optimize the preradiosurgical treatment planning for meningiomas. The concurrent ^{18}F-FDG PET and MR images were less helpful for monitoring the therapeutic response in respect to tumor metabolism. Adverse radiation effect with blood–brain barrier breakdown and perilesional edema

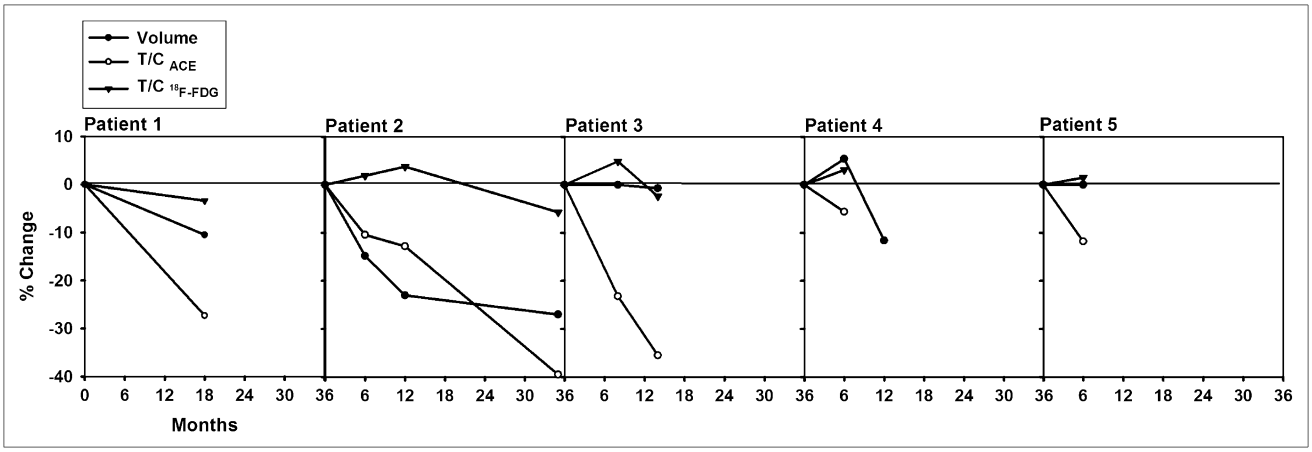

FIGURE 6. Percentage change of tumor volume and T/C ratios of 1-^{11}C-acetate (T/C_{ACE}) and ^{18}F-FDG ($T/C_{^{18}F\text{-}FDG}$) in 5 meningiomas during 6- to 35-mo period after radiosurgery.

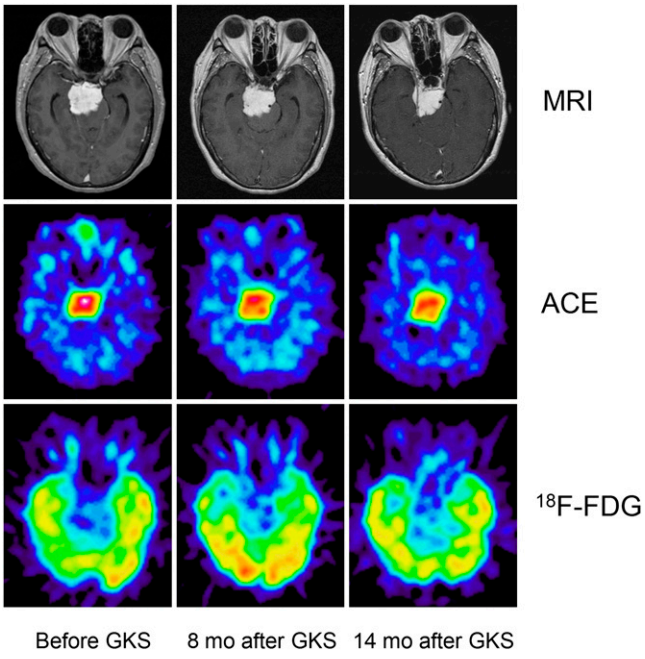

FIGURE 7. Patient 3, parasellar meningioma. Contrast-enhanced MR image showing no obvious change of tumor volume at 8 mo after γ-knife surgery (GKS) but slightly reduced tumor volume at 14 mo. 1-^{11}C-acetate (ACE) PET showing reduction of tumor uptake at 8 mo (−23.2%) and 14 mo (−35.5%) after radiosurgery. ^{18}F-FDG PET showing slightly increased glucose metabolism in tumor (+4.9%) at 8 mo but slightly decreased metabolism (−2.4%) at 14 mo after radiosurgery.

occurred in 4 patients. This effect may explain the enhanced ^{18}F-FDG uptake in the irradiated tumor, which is not uncommonly erroneously interpreted as progression of tumor growth (*44*). 1-^{11}C-acetate seems better than ^{18}F-FDG to reflect the response of tumor metabolism. All 5 patients revealed a decrease of 1-^{11}C-acetate uptake in sequential follow-up PET studies. However, the 1-^{11}C-acetate uptake was persistently higher in tumor than in normal contralateral cortex during the 6- to 35-mo follow-up period, indicating that the tumor growth was arrested rather than eradicated by radiosurgery. Radiation may induce inflammation and gliotic reaction in the brain tumor and peritumoral tissue. The presence of reactive astrocytes minimally affected accumulation of acetate, whereas macrophages enhanced acetate net uptake (*45*). Cellular specificity of acetate uptake and metabolism in brain might be altered by the presence of higher numbers of other cell types in the damaged tissue (*45*). Uptake of 1-^{11}C-acetate by these cells in the irradiated meningioma may sometimes confuse us in the determination of whether the tumor growth is arrested. The evidence from the limited number of cases in the current study suggests that 1-^{11}C-acetate has the potential to be used as a metabolic marker for evaluating the tumor response to radiosurgery, but the current evidence is not enough to conclude the usefulness of 1-^{11}C-acetate in determining tumor viability after radiosurgery. Further investigations are required.

Increased uptake of 1-^{11}C-acetate was found in 1 case of meningeal tuberculoma, which indicates that PET with 1-^{11}C-acetate may not be helpful in the differentiation of meningioma and meningeal tuberculoma. Inflammatory cells, especially macrophages, in the tuberculoma may be responsible for increased uptake of 1-^{11}C-acetate. However, combined labeled acetate and ^{18}F-FDG might provide a new brain imaging application for the assessment of meningeal inflammation and other inflammatory diseases of the brain to provide useful information for localization and characterization of the diseased tissues that require a different intervention.

The major disadvantage of 1-^{11}C-acetate PET is the short half-life of ^{11}C, which requires that PET studies be close to the cyclotron facilities. Labeling of acetate with ^{18}F is a potential means to make possible the clinical use of radiolabeled acetate (*39,46*). Fluoroacetate is the toxic ingredient of the South African poison plant *Dichapetalum chymosum* and of other *Dichapetalum* plants (*47*). Fluoroacetate and its toxic metabolite fluorocitrate inhibit aconitase in brain tissue and are preferentially taken up by glial cells and lead to inhibition of the glial tricarboxylic acid cycle (TCA cycle). Both fluoroacetate and fluorocitrate have been used in in vitro studies with brain slices or cell cultures (*48*). Consequently, ^{18}F-fluoroacetate might be a potential tracer for brain tumor imaging. A minor drawback of 1-^{11}C-acetate in the investigation of meningiomas is that the observation is a little complicated by the low uptake in normal brain structures. Coregistration of 1-^{11}C-acetate PET with MR images would be helpful for visualizing the position of the abnormal 1-^{11}C-acetate uptake.

CONCLUSION

We have evaluated the metabolic activity of meningiomas using 1-^{11}C-acetate and ^{18}F-FDG. 1-^{11}C-acetate was found to be useful for detecting meningiomas and evaluating the extent of meningiomas and potentially useful for monitoring the tumor response to radiosurgery; 1-^{11}C-acetate was, however, found to be not useful for evaluating the histologic grade. In addition, 1-^{11}C-acetate PET permits sharp outlining of meningiomas of various histologic grades and may therefore allow more accurate tumor delineation. This implies that 1-^{11}C-acetate PET is of potential value for guiding the stereotactic biopsy and for optimizing treatment planning before radiosurgery. ^{18}F-FDG was found to be less useful than 1-^{11}C-acetate for evaluating the extent of meningiomas and treatment response of radiosurgery but may be useful for differentiating between benign and malignant meningiomas. Regional accumulation of ^{18}F-FDG and 1-^{11}C-acetate in meningioma dissociates from each other, indicating the diversity of cell metabolism. Both tracers are complementary for assessing the metabolic behavior of meningioma.

ACKNOWLEDGMENTS

We thank the staff of the National PET/Cyclotron Center, Taipei Veterans General Hospital; Chi-Wei Chang, Bang-Hung Yang, and Kuo-Liang Chou for their excellent contribution in providing tracers and in imaging patients; Kuan-Hung Lin, Chih-Hao Chen, Chien-Feng Lin, Ling Chang, and Tsuey-Ling Jan for assistance in preparing the manuscript; and Pui-Ching Lee for consultation on the statistical analysis. This study was supported by National Science Council, Taiwan, under grants NSC86-2314-B075-090, NSC87-2314-B075-004, and NSC91-3112-P-075-001-Y, and by Taipei Veterans General Hospital, under grant V98C1-035.

REFERENCES

1. Black PM. Brain tumors (second of two parts). *N Engl J Med.* 1991;324:1555–1564.
2. Rausing A, Ybo W, Stenflo J. Intracranial meningioma: a population study of ten years. *Acta Neurol Scand.* 1970;46:102–110.
3. Quest Do. Meningiomas: an update. *Neurosurgery.* 1978;3:219–225.
4. Carella RJ, Ransohoff J, Newell J. Role of radiation therapy in the management of meningioma. *Neurosurgery.* 1982;10:332–339.
5. Coke CC, Corn BW, Werner-Wasik M, Xie Y, Curran WJ Jr. Atypical and malignant meningiomas: an outcome report of seventeen cases. *J Neurooncol.* 1998;39:65–70.
6. Di Chiro G. Positron emission tomography using [^{18}F]fluorodeoxyglucose in brain tumors: a powerful diagnostic and prognostic tool. *Invest Radiol.* 1987;22:360–371.
7. Therapeutics and Technology Assessment Subcommittee of the American Academy of Neurology. Assessment: positron emission tomography. *Neurology.* 1991;41:163–166.
8. Warburg O. On the origin of cancer cells. *Science.* 1956;123:309–314.
9. Mahaley MS Jr. In vitro respiration of normal brain and brain tumors. *Cancer Res.* 1966;26:195–197.
10. Ericson K, Lilja A, Bergstrom M, et al. Positron emission tomography with [11-C-methyl]-L-methionine, [11-C]-D-glucose and [68-Ga]EDTA in supratentorial tumors. *J Comput Assist Tomogr.* 1985;9:683–689.
11. Di Chiro G, Hatazawa J, Katz DA, Rizyoli HV, De Michele DJ. Glucose utilization by intracranial meningiomas as an index of tumor aggressivity and probability of recurrence: a PET study. *Radiology.* 1987;164:521–526.
12. Cremerius U, Bares R, Weis J, et al. Fasting improves discrimination of grade 1 and atypical or malignant meningioma in FDG-PET. *J Nucl Med.* 1997;38:26–30.
13. Delbeke D, Myerowitz C, Lapidus RI, et al. Optimal cutoff levels of F-18-fluorodeoxyglucose uptake in differentiation of low-grade from high grade brain tumors with PET. *Radiology.* 1995;195:47–52.
14. Gudjonsson O, Blomquist E, Lilja A, Ericson H, Bergström M, Nybrg G. Evaluation of the effect of high-energy proton irradiation treatment on meningioma by means of ^{11}C-L-methiomine PET. *Eur J Nucl Med.* 2000;27:1793–1799.
15. Pauleit D, Floeth F, Hamacher K, et al. *O*-(2-[^{18}F] Fluoroethyl-L-tyrosine PET combined with MRI improves the diagnostic assessment of cerebral gliomas. *Brain.* 2005;128:678–687.
16. Pruim J, Willemsen ATM, Molenaar WM, et al. Brain tumors: L-[1-C-11] tyrosine PET for visualization and quantification of protein synthesis rate. *Radiology.* 1995;197:221–226.
17. Shinoura N, Nishijima M, Hara T, et al. Brain tumors: detection with C-11 choline PET. *Radiology.* 1997;202:497–503.
18. Shreve P, Chiao PC, Humes D, Schwaiger M, Gross MD. Carbon-11-acetate PET imaging in renal disease. *J Nucl Med.* 1995;36:1595–1601.
19. Yeh SH, Liu RS, Wu LC, et al. ^{11}C-acetate clearance in nasopharyngeal carcinoma. *Nucl Med Commun.* 1999;20:131–134.
20. Oyama N, Akino H, Kanamaru H, et al. ^{11}C-acetate PET imaging of prostate cancer. *J Nucl Med.* 2002;43:181–186.
21. Ho CL, Yu SC, Yeung DW. ^{11}C-acetate PET imaging in hepatocellular carcinoma and other liver masses. *J Nucl Med.* 2003;44:213–221.
22. Liu RS, Chang CP, Chu LS, et al. PET imaging of brain astrocytoma with 1-^{11}carbon-acetate. *Eur J Nucl Med Mol Imaging.* 2006;33:420–427.
23. Dienel GA, Popp D, Drew PD, Ball K, Krisht A, Cruz NF. Preferential labeling of glial and meningial brain tumors with [2-^{14}C]acetate. *J Nucl Med.* 2001;42:1243–1250.
24. Kleihues P, Burger PC, Scheithauer BW. The new WHO classification of brain tumors. *Brain Pathol.* 1993;3:255–268.
25. Ho DMT, Hsu CY, Ting LT, Chiang H. Histopathology and MIB-1 labeling index predicted recurrence of meningiomas. *Cancer.* 2002;94:1538–1547.
26. Pike VW, Eakins MN, Allan RM, Selwyn AP. Preparation of [1-^{11}C]acetate: an agent for the study of myocardial metabolism by positron emission tomography. *Int J Appl Radiat Isot.* 1982;33:505–512.
27. Hamacher K, Coenen HH, Stocklin G. Efficient stereospecic synthesis of no-carrier-added [^{18}F]fluoro-2-deoxyglucose using aminopolyester supported nucleophilic substitution. *J Nucl Med.* 1986;27:235–238.
28. Ogawa T, Shishide F, Kanno I, et al. Cerebral gliomas: evaluation with methionine-PET. *Radiology.* 1993;186:45–53.
29. Kaschten B, Stevenaert A, Sadzot B, et al. Preoperative evaluation of 54 gliomas by PET with fluorine-18-fluorodeoxyglucose and/or carbon-11-methionine. *J Nucl Med.* 1998;39:778–785.
30. Hertz L, Peng L, Dienel GA. Energy metabolism in astrocytes: high rate of oxidative metabolism and spatiotemporal dependence on glycolysis/glycogenolysis. *J Cereb Blood Flow Metab.* 2007;27:219–249.
31. Cruz NF, Lasater A, Zielke HR, Dienel GA. Activation of astrocytes in brain of conscious rat during acoustic stimulation: acetate utilization in working brain. *J Neurochem.* 2005;92:934–947.
32. Dienel GA, Schimidt KC, Cruz NF. Astrocyte activation in vivo during graded photic stimulation. *J Neurochem.* 2007;103:1506–1522.
33. Wolfe RR, Jahoor F. Recovery of labeled CO_2 during the infusion of C-1- vs C-2- labeled acetate: implications for tracer studies of substrate oxidation. *Am J Clin Nutr.* 1990;51:248–252.
34. Pouteau E, Maugere P, Darmaun D, et al. Role of glucose and glutamine synthesis in the differential recovery of $^{13}CO_2$ from in fused 2-^{13}C- versus 1-^{13}C-acetate. *Metabolism.* 1998;47:549–554.
35. Goldman S, Levivier M, Pirotte B, et al. Regional glucose metabolism and histopathology of gliomas: a study based on positron emission tomography–guided stereotactic biopsy. *Cancer.* 1996;78:1098–1106.
36. Berl S, Frigyesi TL. Metabolism of ^{14}C-leucine and ^{14}C-acetate in sensorimotor cortex, thalamus, caudate nucleus and cerebellum of the cat. *J Neurochem.* 1968;15:965–970.
37. Dienel GA, Liu K, Cruz NF. Local uptake of ^{14}C-labeled acetate and butyrate in rat brain in vivo during spreading cortical depression. *J Neurosci Res.* 2001;66:812–820.
38. Yoshimoto M, Waki A, Yonekura Y, et al. Characterization of acetate metabolism in tumor cells in relation to cell proliferation: acetate metabolism in tumor cells. *Nucl Med Biol.* 2001;28:117–122.
39. Ponde DE, Dence CS, Oyama N, et al. ^{18}F-Fluoroacetate: a potential acetate analog for prostate tumor imaging—In vivo evaluation of ^{18}F-fluoroacetate versus ^{11}C-acetate. *J Nucl Med.* 2007;48:420–428.
40. Yoshii Y, Waki A, Furukawa T, et al. Tumor uptake of radiolabeled acetate reflects the expression of cytosolic acetyl-CoA synthetase: implications for the mechanism of acetate PET. *Nucl Med Biol.* 2009;36:771–777.
41. Chung JK, Kim YK, Kim SK, et al. Usefulness of ^{11}C-methionine PET in the evaluation of brain lesions that are hypo- orisometabolic on ^{18}F-FDG-PET. *Eur J Nucl Med Mol Imaging.* 2002;29:176–182.
42. Pirotte B, Goldman S, Massager N, et al. Comparison of ^{18}F-FDG and ^{11}C-methioninefor PET-guided stereotactic brain biopsy of gliomas. *J Nucl Med.* 2004;45:1293–1298.
43. Steiner L, Lindquist C, Steiner M. Meningiomas and gamma knife radiosurgery. In: Al-Mefty O, ed. *Meningiomas.* New York, NY: Raven Press, Ltd.; 1991:263–272.
44. Pan DHC, Guo WY, Chung WY, Shian CY, Liu RS, Lee LS. Early effects of gamma knife surgery on malignant and benign intracranial tumors. *Stereotact Funct Neurosurg.* 1995;64(suppl 1):19–31.
45. Cetin N, Ball K, Gokden M, Cruz NF, Dienel GA. Effect of reactive cell density on net [2-^{14}C]acetate uptake into rat brain: labeling of clusters containing GFAP$^+$- and lectin$^+$-immunoreactive cells. *Neurochem Int.* 2003;42:359–374.
46. Liu RS, Chou TK, Chang CH, et al. Biodistribution, pharmacokinetics and PET imaging of ^{18}F-FMISO, ^{18}F-FDG and ^{18}F-FAc in a sarcoma and inflammation-bearing mouse model. *Nucl Med Biol.* 2009;36:305–312.
47. Morrison JF, Peters RA. Biochemistry of fluoroacetate poisoning: the effect of fluorocitrate on purified aconitase. *Biochem J.* 1954;58:473–499.
48. Fonnum F, Johnsen A, Hassel B. Use of fluorocitrate and fluoroacetate in the study of brain metabolism. *Glia.* 1997;21:106–113.